Journal of the European Ceramic Society 22 (2002) 2877–2882

www.elsevier.com/locate/jeurceramsoc

Depth profiling of a functionally graded alumina/calcium-hexaluminate composite using grazing incidence synchrotron-radiation diffraction

M. Singh, I.M. Low*, D. Asmi

Materials Research Group, Department of Applied Physics, Curtin University, of Technology PO Box U1987 Perth, 6845 WA Australia

Received 28 December 2001; accepted 24 March 2002

Abstract

Grazing incidence synchrotron radiation diffraction (GISRD) has been successfully used for near-surface depth profiling of phase composition, texture and residual strains in a functionally-graded alumina/calcium-hexaluminate (CA_6) composite prepared by infiltration process. Depth profiling of near surface information both in the nanometre and micrometre ranges have been done by using angles of incidence below and above the critical angle (α_c) for total external reflection. The penetration depth increased to several hundred angstroms as α approached α_c. Above α_c there was a rapid increase in penetration depth to a thousand angstroms or more. As the penetration depth increased the intensity of CA_6 peaks relative to those of alumina became less intense, indicating a distinct gradation in the phase abundance. The distribution of CA_6 grains at the near-surface was highly textured and showed a distinct depth-dependent gradation in texture. The presence of graded residual strains in the composite due to thermal expansion mismatch between the phases has been computed and verified from the display of line shifts. The unique but powerful capability of GISRD as a complementary tool for depth profiling the near-surface information of graded materials has been demonstrated in this work.

Keywords: Al_2O_3; $CaAl_{12}O_{19}$; Functionally graded materials; Residual strains; Synchrotron radiation; Texture

1. Introduction

Calcium-hexaluminate, CA_6 (hibonite or $CaAl_{12}O_{19}$) is a layered compound having the magnetoplumbite structure that consists of spinel blocks and conduction layers, which are stacked alternatively to form a layered structure. Spinel blocks are composed only of Al^{3+} and O^{2-} ions, and have the same rigid structure as spinel. Large cations such as Ca^{2+} are usually located in the spacious conduction layer, which has a mirror symmetry plane.[1,2] Depending on the processing route, the morphology of CA_6 grains formed can be either plate-like or equiaxed.[3–5]

In recent years, Al_2O_3–CA_6 composites have been widely studied as structural materials since it was found that Al_2O_3 containing plate-like CA_6 grains showed a more pronounced R-curve behaviour than a composite containing equiaxed grains.[6,7] It has been shown that the increase in aspect ratio of CA_6 grains increases the crack growth resistance, and the crack morphology is planar when CA_6 grains are equiaxed, and tortuous when they are plates.

Layered-graded Al_2O_3–CA_6 composites with unique properties have been recently produced with success by Low and co-workers using an infiltration technique.[8–13] These layered composites, comprising of a homogenous Al_2O_3 layer and a heterogenous layer of Al_2O_3–CA_6 are formed by controlled infiltration of precursors into a porous preform and subsequent firing to form the desired phases. The heterogenous layer in the composite is designed to give functional gradation in composition to minimize the undesirable effect of induced residual stresses that may cause cracking and hinder the process of densification. Depth profiling of phase composition, texture and residual strains in this system is particularly of importance as these are expected to have a profound influence on the mechanical performance of the composite as a whole.

* Corresponding author. Tel.: +61-8-9266-7544; fax: +61-8-9266-2377.

E-mail address: rlowim@cc.curtin.edu.au (I.M. Low).

0955-2219/02/$ - see front matter
PII: S0955-2219(02)00056-0

X-ray diffraction has been previously used by Low and co-workers for depth profiling of phase composition in various layered and graded ceramic systems.[8,9,14–16] This is usually done by gradual polishing or cutting thin slices ~1 mm thick and performing XRD on its surface. However, the information obtained in this case is from a depth of few micrometers from the surface. Hence, it is impossible to depth profile the information on composition, texture and residual strains in these materials at the nanometre scale using conventional XRD. In order to allow in-situ measurement on near-surface on a nanometre scale, grazing angles of incidence are used which allow the penetration of the beam to be varied by variation of the angle of incidence.[17–19]

Lim et al.[19] have demonstrated that surfaces of solids can be studied to advantage by using a highly collimated beam of X-rays striking the surface at a grazing angle near or within the range at which total external reflection occurs. In this situation only the near-surface layer is illuminated and a diffraction pattern is produced which reveals the structure of the surface region in preference to that of the interior. Synchrotron sources are particularly well suited for providing the highly collimated radiation with necessary intensity.[20] The wavelength can be selected to avoid fluorescent background and to obtain highest possible peak to background. The beam broadening due to asymmetric geometry will not lead to peak broadening if the diffraction angle is determined by a set of parallel foils or an analyser crystal in front of the detector.

Going from symmetric diffraction to lower angles of incidence reduces the penetration depth and thus contribution of the near-surface layers. At grazing incidence not only the intensities but also the peak positions (due to refraction) and peak widths (due to total reflection) are changed. Furthermore, the drastic reduction of the penetration depth as the angle of total reflection leads to a steep decrease in intensity from the layers below this interface.

In the present paper, we describe the use of grazing incidence synchrotron radiation diffraction (GISRD) as a powerful tool for depth profiling the near-surface composition, texture, and residual strains of a functionally graded Al_2O_3–CA_6 composite both at a nanometre and micrometre range through the use of angles of incidence below and above the critical angle for total external reflection. Residual strains at different depths from the surface was computed from line shifts due to thermal expansion mismatch between the phases in the graded composite.

2. Experimental procedure

2.1. Preparation of graded alumina/calcium hexaluminate composite

Reactive alumina powder of 0.4 μm average particle size and 99.9% purity from Mandoval UK was used to fabricate alumina preforms for infiltration processing. The as-received powder was pressed into discs of 19 mm diameter and 2 mm thickness at a pressure of 75 MPa, and then pre-sintered at a temperature of 1100 °C for 2 h. The resultant preforms had a porosity of ~46%. The preforms were degassed in a vacuum chamber, and then immersed in a saturated solution of calcium acetate for 30 min. Multiple infiltrations were performed for increased retention of the infiltrant. After each infiltration the samples were fired to 600 °C for 2 h for better adherence of the previous infiltrant. The green infiltrated discs were subsequently fired at a rate of 3 °C/min to 1600 °C for 2 h with 2 h of soaking at 1400 in a high temperature furnace (Ceramic Engineering, Model HT 04/17), to facilitate formation of calcium hexaluminate. The cooling rate was 1 °C/min till room temperature.

2.2. Depth profiling using grazing incidence synchrotron diffraction

Near-surface depth profiling by GISRD was performed using the BIGDIFF instrument located at the Photon Factory, Tsukuba, Japan. Imaging plates were used to record diffraction patterns over a period of 20 min. The depth of X-ray penetration into the composite depends on the grazing angle of incidence α. The grazing incidence angles used were 0.1, 0.3, 0.5, 0.7, 1.0, 3.0, 5.0 and the wavelength used was 1 Å. For calculating the depth of penetration of the beam into the sample, it is necessary to calculate first the critical angle α_c for total external reflection to occur, as follows:[19,20]

$$\alpha_c \approx (2\delta)^{1/2} = 1.6 \times 10^{-3} \rho\lambda \quad (1)$$

where, ρ is density in g/cm^3, λ is wavelength in Å, and $\delta = 1 - n$ for refractive index n. The penetration depth is then calculated from the following equations.[20] For angle of incidence $\alpha < \alpha_c$, penetration depth l is given by:

$$l = \frac{\lambda}{2\pi\left(\alpha_c^2 - \alpha^2\right)^{1/2}} \quad (2)$$

and for $\alpha > \alpha_c$, penetration depth l is given by:

$$l = \frac{2\alpha}{\mu} \quad (3)$$

where μ is the linear attenuation coefficient.[21]

Near surface depth profiles were studied qualitatively from the grazing incidence synchrotron radiation data. For $\lambda = 1$ Å and $\rho = 3800$ kg m^{-3}, the critical angle was calculated as $\alpha_c = 0.348$

As the index of refraction of X-rays is slightly less than unity, the peaks shift to higher angles than those calculated from the Bragg law. For small incidence

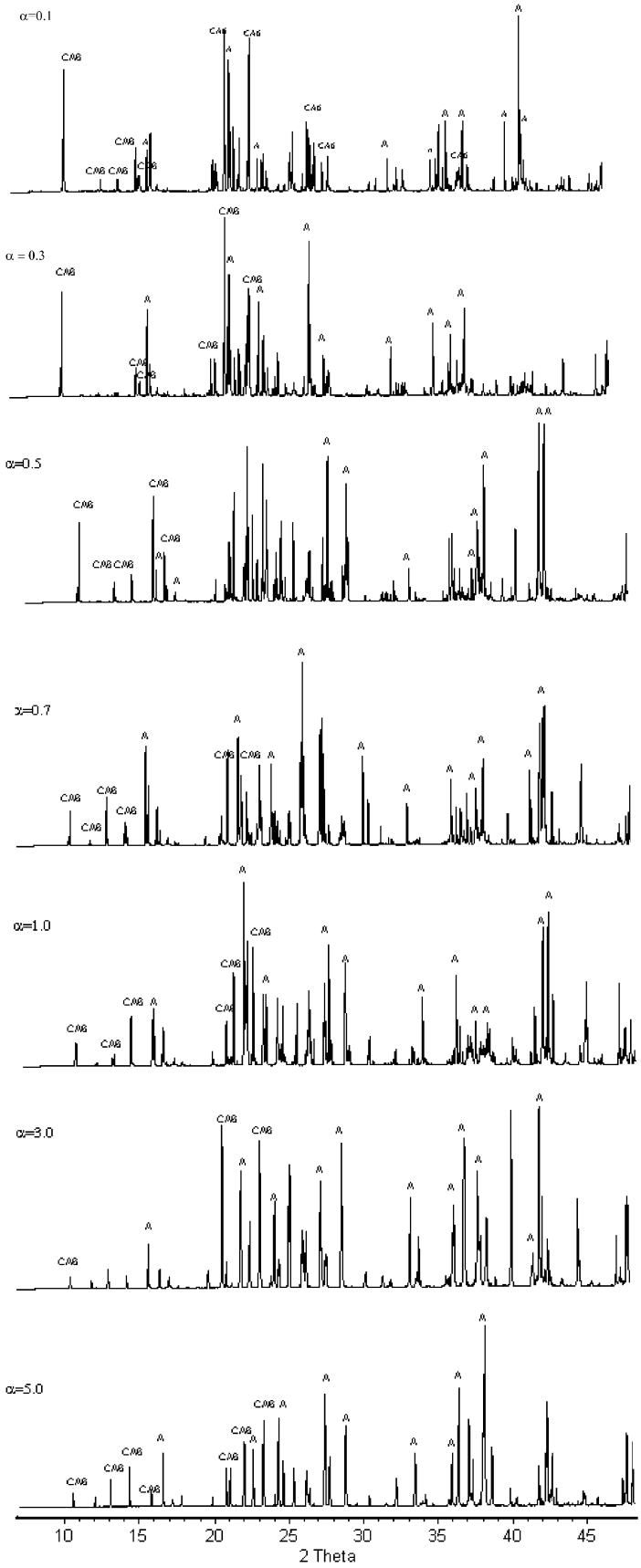

Fig. 1. SRD patterns of graded A/CA_6 sample at different grazing incidence angles.

angles the Bragg angle shift from refraction is given by:[19]

$$\Delta 2\Theta = \frac{\delta}{\sin 2\Theta_{\text{ref}}} \times \left(2 + \frac{\sin\alpha}{\sin 2\Theta_{\text{ref}}} + \frac{\sin 2\Theta_{\text{ref}}}{\sin\alpha}\right) \quad (4)$$

$$2\Theta_{\text{corr}} = 2\Theta_{\text{obs}} - \Delta 2\Theta \quad (5)$$

where, $2\Theta_{\text{corr}}$, $2\Theta_{\text{obs}}$ and $2\Theta_{\text{ref}}$ are the corrected, observed and reference values respectively. After subtracting the refraction shift from observed value the corrected d values (d_{corr}) are obtained. Residual strain arising due to thermal expansion mismatch between the phases in the composite may also contribute to line shifts. Hence, residual strain may then be calculated as follows.

$$\%\ \text{Strain} = \frac{d_{\text{ref}} - d_{\text{corr}}}{d_{\text{ref}}} \times 100 \quad (6)$$

where, d_{ref} is the d value of the strain free powder reference sample of alumina or calcium hexaluminate.

3. Results and discussion

The near-surface diffraction profiles as obtained from SRD at various grazing incidence angles are shown in Fig. 1. The calculated penetration depths at the corresponding grazing incidence angles are shown in Fig. 2. The results indicate that increasing α to just below α_c increased the depth to some hundreds of Angstroms. Above α_c the penetration was inversely proportional to μ and increased to several thousands of angstroms. Small changes in α cause large variations in depth interval, and depth profiling cannot be sensitively controlled at the nanometre scale. However, this provides a depth profile on a larger micrometer scale.

Fig. 3 shows the ratio of peak intensity counts of selected lines of calcium hexaluminate (CA_6), and alumina (A). Lines which were found to be least sensitive to preferred orientation effects [$2\theta = 10.6$ (004) and 33.1 (024) for CA_6 and alumina respectively], have been chosen for this purpose. As the angle of incidence or depth increases, the overall CA_6 features become less intense as compared to alumina. CA_6 intensity ratio curve shows a sharp fall from surface to about 10 μm, below which it plateaus off. This may be indicative of a gradation of composition in the material as expected in an infiltration process. The near-surface layer about 10 μm, is richer in CA_6, but there is a rapid decrease in abundance with depth which levels off gradually at depths greater than 0.1mm from the surface. The graded distribution of CA_6 grains at the near-surface in the microstructure is clearly revealed in Fig. 4. The unique but powerful capability of GISRD as a complementary tool for depth-profiling the near-surface information of graded materials is clearly demonstrated in this work.

It is interesting to note the display of line-shifts associated with all peaks as the grazing angle increased from 0.1 to 5°. As previously highlighted, this phenomenon can be partly attributed to the intrinsic refraction properties of X-rays, causing the peaks to shift to higher angles than those calculated from Bragg's law. The

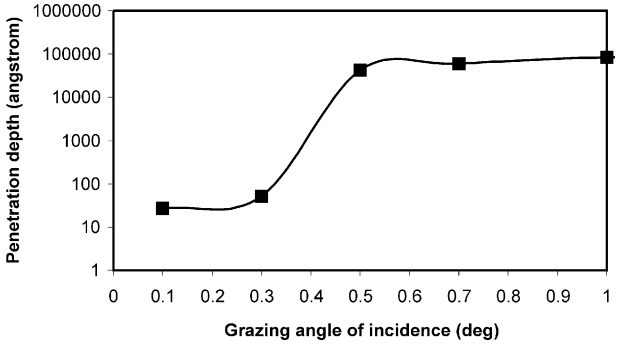

Fig. 2. Penetration depth as a function of grazing-incidence angle.

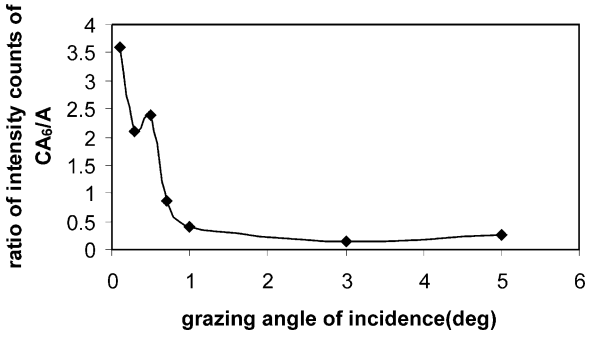

Fig. 3. Ratio of intensity counts of CA_6/A versus grazing-incidence angle.

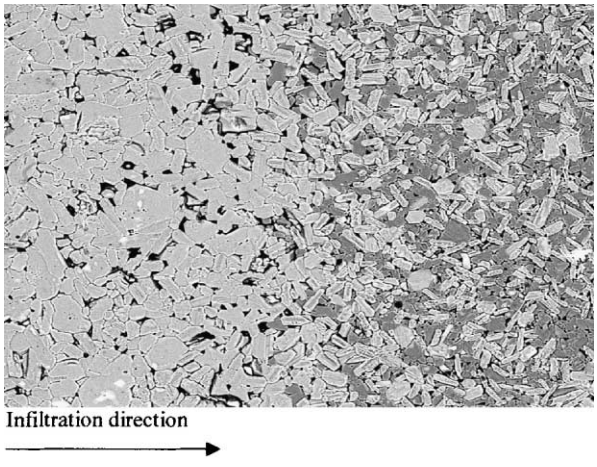

Fig. 4. Back-scattered electron imaging showing the cross-sectional microstructure of graded alumina/CA_6 composite. The light phase is CA_6 and the darker matrix is alumina. The direction of infiltration is from left to right.

presence of residual strains due to thermal expansion mismatch between the phases in the sample can also give rise to line shift. If the sample has a graded distribution of phases, the presence of residual strains will be manifested as line shifts as the grazing angle or surface depth changes.

Eqs. (5) and (6) were used to compute the corrected d spacing taking into account the contribution of line shift due to refraction. The reference d_{ref} and calculated d_{corr} values were used in conjunction with Eq. (7) to compute the amount of residual strains formed in the sample as a result of mismatch in the thermal expansion coefficient between alumina ($\alpha = 8.0\times10^{-6}$ °C^{-1}) and CA_6 ($\alpha = 9.4\times10^{-6}$ °C^{-1}).[13] Fig. 5 shows the plots of residual strains as a function of grazing-incidence angle. It is interesting to note that the variation of residual strains within the alumina matrix, is distinctly depth dependent probably due to the presence of graded CA_6 distribution in the sample. The presence of these surface residual strains in conjunction with the platelet morphology of CA_6 may be responsible for imparting the desirable damage resistance to the otherwise brittle alumina matrix.[6,7]

It can be noted that CA_6 has a pronounced texture as revealed by the variation of intensity ratio for the two maximum intensity lines (107) and (114). According to PDF # 38–0470, for random CA_6 powder, the reference intensity ratio of $I_{(107)}/I_{(114)} = 0.95$. In order to quantify the degree of texture present, the parameter, R, or texture index, is proposed. The value of R is calculated according to the following equation:

$$R = \left[I_{(107)}/I_{(114)}\right]/0.95 \quad (7)$$

When $R = 1.0$, the CA_6 grains are randomly distributed whereas R values greater or lower than 1.0 indicate the presence of preferred grain orientation or texture. The measured values of $I_{(107)}/I_{(114)}$ in Fig. 1 are shown in Table 1. The texture index, R, varies from 1.0 on the top-surface to a maximum value of 2.7 at a depth of 25 μm, indicating the presence of distinct gradation in preferred grain orientation within the layered-graded CA_6 microstructure.

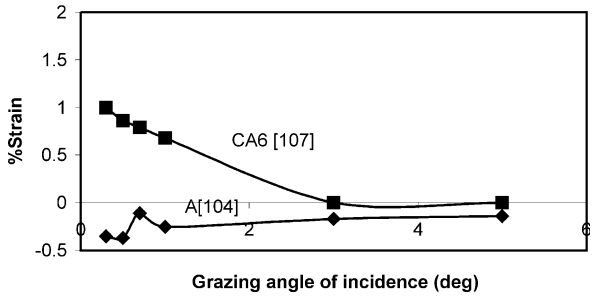

Fig. 5. Plots of residual strains as a function of grazing-incidence angle.

Table 1
Depth-profiling of texture or preferred orientation of CA_6 grains at different grazing-incidence angles

Grazing-incidence angle (°)	$I_{(107)}/I_{(114)}$	Texture index (R)
0.1	0.95	1.0
0.2	1.6	1.7
0.3	1.6	1.7
0.5	1.35	1.4
1	2.56	2.7
3	2.56	2.7
5	0.59	0.6

4. Conclusion

Near-surface depth profiling of phase composition, texture and residual strains in a functionally graded alumina/CA_6 composite has been characterised using grazing-incidence synchrotron radiation diffraction. Results show that the gradation of composition, texture and strains in the composite is continuous even at the nanometre scale. Depth profiling is possible down to several thousand Angstroms in steps of a few Angstroms by changing the incidence angle. Above the critical angle the depth of penetration is several thousand angstroms and depends on the wavelength as well as on the incident angle. The X-ray index of refraction shifts the peaks to higher Bragg angles and these shifts have been calculated using established model. Residual strains at different depths are calculated from line shift by comparing with d values of reference sample.

Acknowledgements

The GISRD data for this work were acquired at the Australian National Beamline Facility at the Photon Factory, Tsukuba, Japan with support from the Australian Synchrotron Research Program (ANBF Proposal 99/2000-AB-26), which is funded by the Commonwealth of Australia under the major National Research Facilities Program. We thank Dr. Garry Foran and Dr. James Hester for technical assistance in data collection. Mr. S. Leung of ANSTO assisted with the work on scanning electron microscopy through funding from AINSE grant. IML is grateful to the Australian Research Council (Project No.: A00001131) for funding this work.

References

1. Kato, K. and Saalfeld, H., Verfeinerung der kristallstruktur von $CaO{\cdot}6Al_2O_3$. *Neues Jahrbuch fuer Mineralogie*, 1968, **109**, 192–200.

2. Utsunomiya, A., Tanaka, K., Morikawa, H., Marumo, F. and Kojima, H., Structure refinement of $CaO.6Al_2O_3$. *J. Solid State Chemistry*, 1988, **75**, 197–200.
3. Criado, E., Pena, P. and Caballero, A., Influence of processing method on microstructural and mechanical properties of calcium hexaluminate compacts. *Science of Ceramic, 1988, 193–198*.
4. De Jonghe, L. C., Schmid, H. and Chang, M., Inter-reaction between Al_2O_3 and $CaO–Al_2O_3$ melt. *J. Am. Ceram. Soc.*, 1984, **67**, 27–30.
5. An, L., Chan, H. M. and Soni, K. K., Control of calcium hexaluminate grain morphology in in-situ toughened ceramic composites. *J. Mater. Sci.*, 1996, **31**, 3223–3229.
6. An, L. and Chan, H. M., R-curve behaviour of in-situ toughened $Al_2O_3/CaAl_{12}O_{19}$ ceramic composites. *J. Am. Ceram. Soc.*, 1996, **79**, 3142–3148.
7. An, L., Chan, H. H. and Chan, H. M., High-strength alumina/alumina-calcium hexaluminate layer composites. *J. Am. Ceram. Soc.*, 1998, **81**, 3321–3324.
8. Low, I. M., Skala, R. D., Asmi, D., Manurung, P. and Singh, M., Infiltration processing of novel functionally graded ceramic materials. In *Proc. 2000 Powder Metallurgy World Congress, 12–16 November*, ed. K. Kosuge and H. Nagai. Kyoto, Japan, 2000, pp. 1465–1468.
9. Asmi, D. and Low, I. M., Processing of an in-situ layered and graded calcium hexaluminate/ alumina composite: I Physical characteristics. *J. Eur. Ceram. Soc.*, 1998, **18**, 2019–2024.
10. Asmi, D. and Low, I. M., Characteristics of layered and graded calcium hexaluminate/alumina composite. *J. Aust. Ceram. Soc.*, 1998, **34**, 152–157.
11. Asmi, D., Low, I. M., Kennedy, S. and Day, A. R., Characteristics of layered and graded calcium hexaluminate/alumina composites. *Mater. Lett.*, 1999, **40**, 96–102.
12. Asmi, D., Low, I. M. and Day, A. R., Physical and microstructural characteristics of HIPed calcium hexaluminate/alumina composites. *J. Aust. Ceram. Soc.*, 1998, **34**, 108–113.
13. Asmi D., *Microstructural Design and Characterisation of Alumina/Calcium–Hexaluminate Composites*. PhD thesis, Curtin University of Technology, Perth, Western Australia, 2001.
14. Low, I. M., Processing of an in-situ layered and graded alumina-aluminium titanate composite. *Mater. Res. Bull.*, 1998, **33**, 1475–1482.
15. Pratapa, S. and Low, I. M., Synthesis and properties of functionally graded aluminium titante/mullite-ZTA composites. *J. Mater. Sci. Lett.*, 1996, **15**, 800–802.
16. Pratapa, S., Low, I. M. and O'Connor, B., Infiltration-processed functionally-graded AT/alumina-zirconia composites: I, microstructural characterisation and physical properties. *J. Mater. Sci.*, 1998, **33**, 3037–3045.
17. Wroblewski, T., Depth profiling using grazing incidence X-ray diffraction. *Mater. Sci. Forum*, 1991, **79**, 469–474.
18. Delhez, R., Keijser, Th.H., Mittemeijer, E. J., Thijsse, B. J., Hollanders, M. A., Loopstra, O. B. and Sloof, W. G., Structure and properties of surface layers: X-ray diffraction studies. *Aus. J. Phy.*, 1988, **41**, 261–282.
19. Lim, G., Parrish, W., Ortish, C., Belletto, M. and Hart, M., Grazing incidence synchrotron diffraction method for analyzing thin films. *J. Mater. Res.*, 1987, **2**, 471–477.
20. Vineyard, G. H., Grazing incidence diffraction and the distorted wave approximation for study of surfaces. *Physical Review B*, 1982, **26**, 4146–4158.
21. ANBF local webpage XCOM.